Modeling Evidence in Support of Coagulative Nucleation Theory

Ashwini Sood, Pankaj Kumar Lodhi

Department of Chemical Engineering, Harcourt Butler Technological Institute, Kanpur 208002, India

Received 21 September 2010; accepted 18 November 2010
DOI 10.1002/app.33778
Published online 27 April 2011 in Wiley Online Library (wileyonlinelibrary.com).

ABSTRACT: An extensive lumped model was developed for emulsion polymerization. It incorporated all of the complex processes: aqueous-phase radical balances for all radical species arising from initiator decomposition and from exit; determination of radical number inside the particles by balance among rates of radical entry into, exit from, and termination inside the particles; determination of the monomer concentration inside the particles and in the aqueous phase by a thermodynamic equation; and particle formation by micellar, homogeneous, and coagulative nucleation. Model validation was done for the system with styrene (monomer), potassium persulfate (initiator), and sodium dodeceyl sulfate (emulsifier) and for the variables, which included the duration of nucleation, conversion at the end of nucleation, and total number of particles formed. The validation process revealed that coagulation during nucleation needed to be included in the model, even for emulsifier concentrations above the critical micelle concentration. The model predictions were in good quantitative agreement with the experimental data. © 2011 Wiley Periodicals, Inc. J Appl Polym Sci 122: 517–531, 2011

Key words: computer modeling; emulsion polymerization; kinetics (polym.); nucleation

INTRODUCTION

Emulsion polymerization follows the kinetics of free-radical-initiated vinyl addition polymerization superimposed on a heterogeneous colloidal latex system. A typical emulsion polymerization reactor, therefore, consists of many components and phases undergoing numerous mass-transfer and reaction processes simultaneously and with strong interactions. The important physical and chemical events in emulsion polymerization include radical generation; chain propagation; chain termination; particle nucleation; the mass transfer of radicals, monomer(s), and emulsifier(s) to and from the latex particles; particle coalescence; and variation of the termination rate constant and propagation rate constant with conversion. A general modeling framework that incorporates all of the relevant mechanisms can be very complex. Much simplicity can be brought about by developing a lumped model, which does not account for the full particle size distribution. Such a model can be developed without the investment of too much time, effort, cost, or computational resources and can serve as a learning model and stepping stone for the development of a more detailed, distributed, or population balance model that accounts for the full particle size distribution.

A mathematical model, based on the population balance approach, was developed for emulsion polymerization.[1] Particle nucleation (micellar) and growth were modeled in adequate detail. The model was validated against the data of Harada et al.[2] for the emulsion polymerization of styrene with water as the dispersion medium, potassium persulfate as the initiator, and sodium dodecyl sulfate as the emulsifier. Variables considered for the model validation were the total number of particles formed, duration of the nucleation period, conversion at the end of nucleation, variation of the monomer volume fraction inside the particles with conversion, and conversion–time curves for different emulsifier, initiator, and monomer concentrations. Close agreement was found between the simulations and the experimental data.

We started this study with the aim of developing a lumped model based on the monodispersed approximation (all of the particles having the same size at a given time) to evaluate some of the assumptions made in the aforementioned model. Aqueous-phase radical termination and radical exit, which were neglected in the previous model, were included in this model. Individual radical balances, which were not incorporated into the previous model, were now incorporated. The dependence of the monomer volume fraction inside the particles on

Correspondence to: A. Sood (sood.ashwini@rediffmail.com).

the particle size and interfacial tension were also included. Different nucleation mechanisms, which included micellar nucleation, homogeneous nucleation, and coagulative nucleation, were sequentially included to assess their effect on the experimental variables. The validation process revealed that the coagulation of the particles during the nucleation period needed to be included to match the simulation results with the experimental data.

PHYSICAL PICTURE

The model simulates an isothermal, well-stirred, batch emulsion polymerization reaction. At the very beginning of the polymerization, the reaction system consists of monomer droplets (ca. 1–10 μm in diameter, 10^{12}–10^{14} dm^{-3} in number) dispersed in the continuous aqueous phase with the aid of the emulsifier.[3] Monomer-swollen micelles (ca. 5–10 μm in diameter, 10^{19}–10^{21} dm^{-3} in number) also exist in the reaction system, provided the concentration of the emulsifier is above its critical micelle concentration. Only a very small amount of relatively hydrophobic monomer is solubilized in the micelles and dissolved in the aqueous phase. The majority of the monomer molecules are present in large monomer droplets. The polymerization is initiated by the addition of an initiator. The radicals generated from the decomposition of the initiator propagate in the aqueous phase, are captured by micelles (and also by particles after nucleation), and terminate in the aqueous phase with other radicals. Monomer droplets, because of their large size and, consequently, relatively small interfacial area are not effective in competing with micelles and particles in capturing free radicals from the aqueous phase. When a free radical enters a micelle and begins to polymerize with the monomer present in it, particle formation or nucleation takes place. This mode of particle nucleation is called *micellar nucleation*. The particles are also generated if the propagating oligomers exceed a critical chain length, depending on their water solubility, and precipitate out of the aqueous phase. The precipitating oligomers may flocculate with other oligomers to acquire necessary colloidal stability. This mode of particle formation is called *homogeneous nucleation*. The particles thus formed grow because of polymerization. It is now suggested that the growing particles, formed by micellar nucleation, homogeneous nucleation, or both, undergo coagulation during the nucleation stage. This mode of nucleation, involving the coagulation of newly formed particles, is called *coagulative nucleation*. The monomer is transported to the growing particles from the monomer droplets by diffusion through the aqueous phase. The free radicals enter the particles intermittently, and their number is governed by the balance between the rates of radical entry into, exit from, and termination inside the particles. In a typical emulsion polymerization reactor, the aqueous-phase radical concentration is about 10^{15} number/dm^3. The number of particles is about 10^{17} number/dm^3. Thus, there is 1 radical per 100 particles. The exit of radicals may take place during polymerization. Radical exit proceeds by a stepwise mechanism involving discrete processes. The first is the transfer of free-radical activity from a growing polymer chain to a monomer molecule. The monomeric radical so formed is highly mobile and may diffuse to the surface of the particle before the addition of one or more monomer molecules. From the surface of the particles, the radical may diffuse away from the surface into the bulk of the aqueous phase. The exited radicals may propagate in the aqueous phase, be captured by the micelles and the particles, or terminate with other aqueous-phase radicals. To maintain the adequate colloidal stability of the growing particles, micelles that do not contribute to the particle nucleation give up their emulsifier to supply the increasing demand of emulsifier on the growing particle interfacial area. The particle nucleation stage (interval I) ends immediately after all of the micelles are depleted. About 1 of every 100–1000 micelles can be successfully converted into latex particles. The rest disband to give their emulsifier to stabilize the growing particle interfacial area. After the particle nucleation is completed, the number of latex particles or reaction loci remains relatively constant until the end of polymerization. The particles grow in size because of polymerization. The monomer droplets serve as reservoirs to supply the growing particles with monomer. The majority of the monomer is consumed in the particle growth stage, which ranges from about 10–20 to 60% monomer conversion. The particle growth stage (interval II) ends when monomer droplets disappear from the reaction system. In interval III, the particles become monomer-starved, and the concentration of the monomer in them decreases until the end of polymerization. The polymerization rate begins to decrease. The polymerization rate may increase drastically with increasing conversion; this is attributed to the greatly reduced bimolecular termination between two polymeric radicals in the very viscous reaction loci when the polymerization is carried out at a temperature below the glass-transition temperature of the monomer–polymer solution. This phenomenon is called *auto-acceleration*, or the *Trommsdorff effect*.

OVERALL REACTOR BALANCES

The overall reactor balances include the material balance for the polymer and initiator and the balances for the volume of the reactor and the total number

of particles formed. The material balances, which express the rate of change of moles of polymer and initiator, contain accumulation and reaction terms. The volume of the reactor changes because of the density differences between the monomer and the polymer. The number of particles changes because of the nucleation of the particles, as shown in the following equations:

$$\frac{d[\mathrm{P}]_R V_R}{dt} = R_P V_R \tag{1}$$

where $[\mathrm{P}]_R$ is the polymer concentration in the reaction medium (mol/cm^3), V_R is the volume of the reaction medium (cm^3), t is time (s), and R_P is the rate of polymerization (mol/s):

$$R_P = k_p \frac{\rho_M}{\mathrm{MW}_M N_A} N_P \Phi i$$

where k_p is the propagation rate constant in the particles (cm^3 mol^{-1} s^{-1}), ρ_M is the density of the monomer (g/cm^3), MW_M is the molecular weight of the monomer (g/mol), N_A is Avogadro's number, N_P is the total number of particles formed, Φ is the monomer volume fraction inside the particles, and i is the average number of radicals per particle.

$$\frac{d[\mathrm{I}]_W V_W}{dt} = -k_d [\mathrm{I}]_W V_W \tag{2}$$

where $[\mathrm{I}]_W$ is the initiator concentration in the aqueous phase (mol/cm^3), V_W is the volume of the aqueous phase (cm^3), k_d is the initiator decomposition rate constant (s^{-1}).

$$\frac{dV_R}{dt} = -\left(\frac{1}{\rho_M} - \frac{1}{\rho_p}\right) R_P \mathrm{MW}_M \tag{3}$$

where ρ_p is the density of the polymer (g/cm^3).

$$\frac{dN_P}{dt} = R_{\mathrm{nuc}} \tag{4}$$

where R_{nuc} is the rate of nucleation (s^{-1}).

The evaluation of the rate of nucleation is discussed in the next section. The evaluation of the rate of polymerization required the values of the monomer volume fraction inside the particles and the average number of radicals per particle. Their evaluation is also discussed later.

RATE OF NUCLEATION

Many mechanisms have been proposed for particle nucleation in conventional or macroemulsion polymerization. The important ones are nucleation in monomer-swollen micelles, nucleation in the aqueous phase, or homogeneous nucleation and coagulative nucleation. A review of these mechanisms can be found elsewhere.[1]

The micellar nucleation mechanism, postulated by Harkins[4,5] and quantified by Smith and Ewart,[6] comprises particle formation by the entry of radicals, generated in the aqueous phase, into the monomer-swollen micelles. The nucleation is over when all of the micelles have been transformed into polymer particles or have given up their monomer and emulsifier to growing particles.

In the homogeneous nucleation theory or nucleation in the aqueous phase, the radicals generated in the aqueous phase add monomer molecules dissolved in the aqueous phase until the oligomeric radicals so formed exceed their solubility in the aqueous phase and precipitate. The precipitating radicals either nucleate a particle by adsorbing emulsifier molecules and absorbing monomer molecules or flocculate among themselves or particles already formed. Flocculation develops until a critical surface potential develops to prevent further flocculation. A surface charge is provided by the initiator end groups and emulsifier molecules. This mechanism was proposed independently by Priest[7] and Jacobi[8] and was developed further by Fitch and Tsai.[9] Hansen and Ugelstad[10] proposed that the free radicals in the aqueous phase propagate with the dissolved monomer. When a critical chain length is reached, primary particles form by precipitation. Before growth from a free radical to a primary particle, each oligomer can (1) terminate with other radicals, (2) precipitate if its chain length exceeds the critical chain length, or (3) be captured by the particles and micelles (if present). Maxwell et al.[11] suggested that the values to be used for the critical chain length are much smaller than that originally thought and gave a value of 5 for styrene.

A relatively recent development is the idea of coagulative nucleation theory, which may be thought of as an extension to the micellar and the homogeneous nucleation mechanisms. According to this mechanism, proposed by Lichti et al.[12] and Feeney et al.,[13] the formation of a stable polymer particle occurs in a two-step process. The first step involves the formation of colloidally unstable precursor particles through either micellar or homogeneous nucleation. This is followed by a second step, involving the coagulation of these precursor particles to form stable true or mature particles. This theory is based on the positive skewness of the particle size distribution as a function of volume during interval II. This implies that the rate of nucleation in interval I increases with time until it drops with the cessation of nucleation. The authors claimed that micellar

nucleation and homogeneous nucleation incorrectly predict either decreasing or constant nucleation rates.

The rate of micellar nucleation is given by the rate of radical entry into micelles. Radical entry into micelles (and particles) has been postulated to take place via different mechanisms, the important ones being radical entry due to propagation in the aqueous phase,[11] radical entry due to diffusion,[14] and radical entry due to collision.[15] In this article, the rate of radical entry into the micelles (R_{em}; s^{-1}) is given as follows:

$$R_{em} = k_{mm} A_m R_{\text{tot}} \tag{5}$$

where k_{mm} is the mass-transfer coefficient of radical entry into the micelles (cm^{-2} s^{-1}), A_m is the total surface area of the micelles (cm^2), and R_{tot} is the total aqueous-phase radical concentration (mol/cm^3). Here, we use the collisional radical entry model, as we have done in our previous studies.[1,16–19]

According to the propagational entry model, only radicals derived from water-soluble initiators with a chain length above a critical degree of polymerization (2–3 for styrene) can enter the particles. However, there now exists experimental evidence provided by Tauer et al.[20] that persulfate radicals also enter the particles. They reported in their article that any kind of radical that is present in the aqueous phase can enter the particles with a probability proportional to its concentration. Thus, both primary initiator radicals and oligomeric radicals can enter the particles. There is obviously no preference of the particles to allow only a special sort of radicals to enter.

These different entry models give different particle size dependencies of the entry rate coefficient. Although the propagational entry model gives that the first-order entry rate coefficient is independent of the particle radius, the diffusional entry model gives that the entry rate coefficient is proportional to the particle radius varying from 1 to 3 power, and the collisional entry model gives that the entry rate coefficient is proportional to the square of the particle radius. Hernandez and Tauer[21] showed that the Smoluchowski equation for diffusion-controlled reactions, which assumes that one particle is dispersed in an infinite medium, is applicable for a very low number concentration of particles, for small particle diameters, and therefore, for low dispersed-phase volume fractions. A significant deviation from this equation was reported for a high particle number concentrations and large diameters or for high dispersed-phase volume fractions. They confirmed that only for very dilute dispersions could entry rate coefficients be represented by the Smoluchowski equation. They pointed out that when the collision rate coefficient is expressed as a function of the particle diameter, depending on the range of values for the number concentration and size of the particles, different functional dependencies of the entry rate coefficient on the particle diameter were observed; these ranged from a linear to a forth-power relationship. This means that the effect of the dispersed-phase volume fraction on the collision kinetics under diffusion-controlled conditions could explain the different results obtained during the determination of radical entry coefficients in emulsion polymerization. The authors suggested that the precise determination of the radical entry mechanism can be reliable only if a wide range of values for the dispersed-phase volume fraction, from very diluted (0.1%) to concentrated (>10%) dispersions, is considered.

The total surface area of the micelles in the previous equation is calculated from

$$A_m = A_{m0} - A_P, \text{ if } \quad A_m > 0 \tag{6}$$

where A_{m0} is the total initial surface area of the micelles (cm^2) and A_P is the total particle surface area (cm^2). Otherwise, when $A_m = 0$.

$$A_{m0} = m_e / \text{MW}_E N_A a_{em} \tag{7}$$

where m_e is the mass of the emulsifier in the reaction medium (g) MW_E is the molecular weight of the emulsifier (g/mol), and a_{em} is the emulsifier surface coverage area on the micelles (cm^2/molecule). Also

$$A_P = N_P 4\pi r^2 \tag{8}$$

where r is the radius of the particle (cm).

The radius of the particle is calculated as follows:

$$v_P = [\text{P}]_R V_R \text{MW}_M / [N_P \rho_p (1 - \Phi)] \quad \text{and} \quad r = (3v_P/4\pi)^{\frac{1}{3}} \tag{9}$$

where v_P is the volume of a particle (cm^3).

The rate of homogeneous nucleation (R_{hom}; s^{-1}) is given in this study as follows:

$$R_{\text{hom}} = k_p [\text{M}]_{\text{aq}} (R_5 + M_5) \tag{10}$$

where $[\text{M}]_{\text{aq}}$ is the monomer concentration in the aqueous phase (mol/cm^3), R_i is the total aqueous-phase concentration of a radical with chain length i derived from the initiator decomposition (mol/cm^3; $= 1, 2, 3, 4,$ or 5), and M_i is the aqueous-phase concentration of a radical with chain length i derived from the exited radical (mol/cm^3; $i = 1, 2, 3, 4,$ or 5). The rate of coagulative nucleation (R_{coag}; s^{-1}) in this study is given as follows:

$$R_{\text{coag}} = -\beta N_P^2 \tag{11}$$

where β is coagulation rate constant (number of particles)$^{-1}$ s^{-1}. It was treated as an adjustable parameter in this study.

Thus, R_{nuc} is given as the sum of all of these nucleation rates:

$$R_{nuc} = R_{em} + R_{hom} + R_{coag} = k_{mm}A_mR_{tot} + k_p[M]_{aq}(R_5 + M_5) - \beta N_P^2 \quad (12)$$

The calculation requires R_{tot}, the concentration of an oligomeric radical of chain length 5 initiated from the initiator radical (R_5), and the concentration of an oligomeric radical of chain length 5 initiated from the exited monomeric radical (M_5). Their calculations are discussed next.

AQUEOUS-PHASE RADICAL BALANCES

The aqueous-phase radical balances consist of balances for radicals of different chain lengths (up to 5 for styrene) derived from the initiator decomposition and their further propagation in the aqueous phase and also from exited radicals and their further propagation in the aqueous phase.

Writing the steady-state balances for initiator radicals and oligomers derived from their further propagation by reaction with the dissolved monomer in the aqueous phase, we get the following balance equations for each:

$$R_1 : 2fk_d[I]_W - k_{pw}[M]_{aq}R_1 - k_{mm}A_mR_1 - k_{mp}A_PR_1 - k_{tw}R_1(R_1 + R_2 + R_3 + R_4 + R_5 + M_1 + M_2 + M_3 + M_4 + M_5) = 0$$

or, $$R_1 : 2fk_d[I]_W - k_{pw}[M]_{aq}R_1 - k_{mm}A_mR_1 - k_{mp}A_PR_1 - k_{tw}R_1(R + M) = 0$$

where $R = R_1 + R_2 + R_3 + R_4 + R_5$ and $M = M_1 + M_2 + M_3 + M_4 + M_5$ (13)

where f is the initiator decomposition efficiency, k_{pw} is the propagation rate constant in the aqueous phase (cm^3 mol^{-1} s^{-1}), k_{mp} is the mass-transfer coefficient of radical entry into the particles (cm^{-2} s^{-1}), k_{tw} is the termination rate constant in the aqueous phase (cm^3 mol^{-1} s^{-1}), R is the total aqueous-phase concentration of radicals derived from the initiator decomposition (mol/cm^3), and M is the total aqueous-phase concentration of radicals derived from exited radicals (mol/cm^3). Similarly, for R_2, R_3, R_4, and R_5, we get

$$R_2 : k_{pw}[M]_{aq}R_1 - k_{pw}[M]_{aq}R_2 - k_{mm}A_mR_2 - k_{mp}A_PR_2 - k_{tw}R_2(R + M) = 0 \quad (14)$$

$$R_3 : k_{pw}[M]_{aq}R_2 - k_{pw}[M]_{aq}R_3 - k_{mm}A_mR_3 - k_{mp}A_PR_3 - k_{tw}R_3(R + M) = 0 \quad (15)$$

$$R_4 : k_{pw}[M]_{aq}R_3 - k_{pw}[M]_{aq}R_4 - k_{mm}A_mR_4 - k_{mp}A_PR_4 - k_{tw}R_4(R + M) = 0 \quad (16)$$

$$R_5 : k_{pw}[M]_{aq}R_4 - k_{pw}[M]_{aq}R_5 - k_{mm}A_mR_5 - k_{mp}A_PR_5 - k_{tw}R_5(R + M) = 0 \quad (17)$$

Writing the balances for exited radicals and oligomers derived from them by further propagation by reaction with the dissolved monomer in the aqueous phase, we get the following equations:

$$M_1 : k_{de}N_Pi - k_{pw}[M]_{aq}M_1 - k_{mm}A_mM_1 - k_{mp}A_PM_1 - k_{tw}M_1(R + M) = 0 \quad (18)$$

$$M_2 : k_{pw}[M]_{aq}M_1 - k_{pw}[M]_{aq}M_2 - k_{mm}A_mM_2 - k_{mp}A_PM_2 - k_{tw}M_2(R + M) = 0 \quad (19)$$

$$M_3 : k_{pw}[M]_{aq}M_2 - k_{pw}[M]_{aq}M_3 - k_{mm}A_mM_3 - k_{mp}A_PM_3 - k_{tw}M_3(R + M) = 0 \quad (20)$$

$$M_4 : k_{pw}[M]_{aq}M_3 - k_{pw}[M]_{aq}M_4 - k_{mm}A_mM_4 - k_{mp}A_PM_4 - k_{tw}M_4(R + M) = 0 \quad (21)$$

$$M_5 : k_{pw}[M]_{aq}M_4 - k_{pw}[M]_{aq}M_5 - k_{mm}A_mM_5 - k_{mp}A_PM_5 - k_{tw}M_5(R + M) = 0 \quad (22)$$

where k_{de} is the radical exit coefficient (s^{-1}). Adding these equations, we note that the propagation terms cancel one another, and only the last propagation terms remain, that is, $k_{pw}[M]_{aq}R_5 + k_{pw}[M]_{aq}M_5$, which is the rate at which oligomers exceeding a chain length of 5 precipitate out of the aqueous phase and, hence, do not contribute to the aqueous-phase radical balance. Also, the radical entry to the micelle terms add up to yield $-k_{mm}A_m(R + M)$, the radical entry to the particles terms add up to yield $-k_{mp}A_P(R + M)$, and the termination terms add up to yield $-k_{tw}(R + M)^2$. Therefore, after adding, we get:

$$2fk_d[I]_W + k_{de}N_Pi - k_{mm}A_m(R + M) - k_{mp}A_P(R + M) - k_{tw}(R + M)^2 = 0 \quad (23)$$

Writing $R + M$ as R_{tot}, we get:

$$2fk_d[I]_W + k_{de}N_Pi - k_{mm}A_mR_{tot} - k_{mp}A_PR_{tot} - k_{tw}R_{tot}^2 = 0 \quad (24)$$

From the previous equations, the individual radical concentrations can be expressed as follows:

$$R_1 = 2fk_d[I]_W/(k_{pw}[M]_{aq} + k_{mm}A_m + k_{mp}A_P + k_{tw}R_{tot}) \quad (25)$$

$$R_2 = k_p[\mathrm{M}]_{\mathrm{aq}} R_1/(k_{pw}[\mathrm{M}]_{\mathrm{aq}} + k_{mm}A_m + k_{mp}A_P + k_{tw}R_{\mathrm{tot}}) = (2fk_d[\mathrm{I}]_W)(k_{pw}[\mathrm{M}]_{\mathrm{aq}}R_1) /(k_{pw}[\mathrm{M}]_{\mathrm{aq}} + k_{mm}A_m + k_{mp}A_P + k_{tw}R_{\mathrm{tot}})^2 \quad (26)$$

Similarly, we have

$$R_3 = (2fk_d[\mathrm{I}]_W)(k_{pw}[\mathrm{M}]_{\mathrm{aq}})^2/(k_{pw}[\mathrm{M}]_{\mathrm{aq}} + k_{mm}A_m + k_{mp}A_P + k_{tw}R_{\mathrm{tot}})^3 \quad (27)$$

$$R_4 = (2fk_d[\mathrm{I}]_W)(k_{pw}[\mathrm{M}]_{\mathrm{aq}})^3 /(k_{pw}[\mathrm{M}]_{\mathrm{aq}} + k_{mm}A_m + k_{mp}A_P + k_{tw}R_{\mathrm{tot}})^4 \quad (28)$$

$$R_5 = (2fk_d[\mathrm{I}]_W)(k_{pw}[\mathrm{M}]_{\mathrm{aq}})^4 /(k_{pw}[\mathrm{M}]_{\mathrm{aq}} + k_{mm}A_m + k_{mp}A_P + k_{tw}R_{\mathrm{tot}})^5 \quad (29)$$

$$M_1 = k_{de}N_P i(k_{pw}[\mathrm{M}]_{\mathrm{aq}} + k_{mm}A_m + k_{mp}A_P + k_{tw}R_{\mathrm{tot}}) \quad (30)$$

$$M_2 = (k_{de}N_P i)(k_p[\mathrm{M}]_{\mathrm{aq}}) /(k_{pw}[\mathrm{M}]_{\mathrm{aq}} + k_{mm}A_m + k_{mp}A_P + k_{tw}R_{\mathrm{tot}})^2 \quad (31)$$

$$M_3 = (k_{de}N_P i)(k_p[\mathrm{M}]_{\mathrm{aq}})^2/(k_{pw}[\mathrm{M}]_{\mathrm{aq}} + k_{mm}A_m + k_{mp}A_P + k_{tw}R_{\mathrm{tot}})^3 \quad (32)$$

$$M_4 = (k_{de}N_P i)(k_{pw}[\mathrm{M}]_{\mathrm{aq}})^3 /(k_P[\mathrm{M}]_{\mathrm{aq}} + k_{mm}A_m + k_{mp}A_P + k_{tw}R_{\mathrm{tot}})^4 \quad (33)$$

$$M_5 = (k_{de}N_P i)(k_{pw}[\mathrm{M}]_{\mathrm{aq}})^4 /(k_{pw}[\mathrm{M}]_{\mathrm{aq}} + k_{mm}A_m + k_{mp}A_P + k_{tw}R_{\mathrm{tot}})^5 \quad (34)$$

Defining $A = 2fk_dI$, $B = k_{pw}[\mathrm{M}]_{\mathrm{aq}}$, $C = (k_{pw}[\mathrm{M}]_{\mathrm{aq}} + k_{mm}A_m + k_{mp}A_P + k_{tw}R_{\mathrm{tot}})$, and $A' = k_{de}N_P i$, we get on adding the following equation:

$$\begin{aligned} R_{\mathrm{tot}} &= (R_1 + R_2 + R_3 + R_4 + R_5 + M_1 + M_2 + M_3 + M_4 + M_5) \\ &= (A/C + AB/C^2 + AB^2/C^3 + AB^3/C^4 + AB^4/C^5) \\ &\quad + (A'/C + A'B/C^2 + A'B^2/C^3 + A'B^3/C^4 + A'B^4/C^5) \\ &= A/C(1 + B/C + B^2/C^2 + B^3/C^3 + B^4/C^4) \\ &\quad + A'/C(1 + B/C + B^2/C^2 + B^3/C^3 + B^4/C^4) \\ &= (A + A')/C(1 + B/C + B^2/C^2 + B^3/C^3 + B^4/C^4) \\ &= (A + A')/C\{[1 - (B/C)^5]/(1 - B/C)\} \end{aligned} \quad (35)$$

Because $B = (k_{pw}[\mathrm{M}]_{\mathrm{aq}}) \ll C = (k_{pw}[\mathrm{M}]_{\mathrm{aq}} + k_{mm}A_m + k_{mp}A_P + k_{tw}R_{\mathrm{tot}})$, $B/C \ll 1$, and $(B/C)^5 \approx 0$, we get

$$R_{\mathrm{tot}} = (A + A')/(C - B)$$

or

$$R_{\mathrm{tot}} = (2fk_dI + k_{de}N_P i)/(k_{mm}A_m + k_{mp}A_P + k_{tw}R_{\mathrm{tot}})$$

or see eq. (24), which is the same as the aqueous-phase radical balance derived before. Here, the dependence of the rate constants on the chain length was neglected.

MONOMER VOLUME FRACTION INSIDE THE PARTICLES

Monomer diffusion into the particles ordinarily occurs at a very fast rate.[22,23] Thus, one can make the quasi-steady-state assumption that monomer concentration inside the particles is at thermodynamic equilibrium at all times. The equilibrium monomer volume fraction can be obtained from eq. (36), given by Min and Ray,[24,25] which is an extension of that developed by Morton et al.[26]

$$2\gamma \mathrm{MW}_M/rR_GT + [1 - \Phi + \ln\Phi - \chi(1 - \Phi)^2] = \ln\{[\mathrm{M}]_{\mathrm{aq}}/[\mathrm{M}]_{\mathrm{sat}}\} \quad (36)$$

where γ is the interfacial tension (dyne/cm), R_G is the universal gas constant (cal mol^{-1} K^{-1}), T is the absolute temperature (K), χ is the Flory–Huggins interaction parameter, and $[\mathrm{M}]_{\mathrm{sat}}$ is the monomer concentration at saturation in the aqueous phase (mol/cm^3).

The previous equation results from the balance between the gain in free energy caused by the increase in the interfacial area on swelling, the loss in free energy caused by mixing of the monomer with the polymer, and the gain in free energy caused by the separation of the monomer from the aqueous phase. This equation is coupled to the monomer balance because of the presence of $[\mathrm{M}]_{\mathrm{aq}}$. $[\mathrm{M}]_{\mathrm{aq}}$ can be determined from the following equation:

$$[\mathrm{M}]_R V_R = [\mathrm{M}]_P V_P + [\mathrm{M}]_D V_D + [\mathrm{M}]_{\mathrm{aq}} V_W \quad (37)$$

where $[\mathrm{M}]_R$ is the monomer concentration in the reaction medium (mol/cm^3), $[\mathrm{M}]_P$ is the monomer concentration in the particles (mol/cm^3), V_P is the volume of the particles (cm^3), $[\mathrm{M}]_D$ is the monomer concentration in the droplets (mol/cm^3) and V_D is the volume of the droplets (cm^3). Alternatively, we can write

$$[\mathrm{M}]_{\mathrm{aq}} V_W = [\mathrm{M}]_R V_R - [\mathrm{M}]_P V_P - [\mathrm{M}]_D V_D$$

The amount of monomer dissolved in the aqueous phase ($[\mathrm{M}]_{\mathrm{aq}}V_W$) is obtained by the difference between the total amount of monomer present in the reactor ($[\mathrm{M}]_R V_R$) and the monomer present inside the particles ($[\mathrm{M}]_P V_P$) and the monomer droplets ($[\mathrm{M}]_D V_D$).

When the monomer droplets are present in the reactor, the aqueous phase is saturated with the

monomer ($[M]_{aq} = [M]_{sat}$). Thus, Φ can be calculated from eq. (36); however, when the droplets are absent ($V_D = 0$), then eqs. (36) and (37) must be solved simultaneously for Φ and $[M]_{aq}$. In that case, $[M]_{aq}$ can be calculated from the following equation:

$$[M]_{aq} V_W = N_{m0}(1 - X) - \Phi/(1 - \Phi) \times N_{m0} X \times \rho_M/\rho_p \tag{38}$$

where N_{m0} is the initial number of moles of the monomer (mol) and X is the conversion. In eq. (36), r is the swollen particle radius. It can be expressed in terms of the unswollen or dry particle radius (r_{dry}) as follows:

$$r = r_{dry}/(1 - \Phi)^{\frac{1}{3}} \tag{39}$$

where r_{dry} is given by

$$r_{dry} = [3/4\pi(N_{m0} X M W_M/\rho_p N_P)]^{\frac{1}{3}} \tag{40}$$

AVERAGE NUMBER OF RADICALS PER PARTICLE

The average number of radicals per particle is determined by the rates of radical entry into, exit from, and termination inside the particle. This is given by the quasi-steady-state eq. (41), which is the Smith–Ewart recursion relation:[6]

$$k_e[F_{i-1} - F_i] + k_{de}[(i+1)F_{i+1} - iF_i] + \frac{k_t}{2v_P N_A}[(i+2)(i+1)F_{i+2} - i(i-1)F_i] = 0 \tag{41}$$

where k_e is the radical entry rate coefficient (s^{-1}), F_i is the number of particles containing i radicals, and k_t is the radical termination rate constant inside the particles ($cm^3\ mol^{-1}\ s^{-1}$).

The Stockmayer–O'Toole solution of the previous equation for the average number of radicals per particle [$i(\nu_P, t)$] is given by the following equation:[27,28]

$$i(\nu_P, t) = \sum_{i=0}^{\infty} \frac{iF_i}{F(v,t)} = \frac{a}{4}\frac{I_b(a)}{I_{b-1}(a)} \tag{42}$$

where $I_b(a)$ is the modified Bessel function of the first kind of order b and argument a, where

$$a = 4\left(\frac{\nu_P N_A k_e}{k_t}\right)^{1/2} \quad \text{and} \quad b = \frac{2\nu_P N_A k_{de}}{k_t} \tag{43}$$

where parameter a accounts for the relative importance of radical entry with respect to radical termination and parameter b accounts for the relative importance of radical exit with respect to radical termination inside the particle.

For this study, the continued fraction form, first used by Ugelstad et al.,[29] was used:

$$i = \frac{a}{4}\frac{I_b(a)}{I_{b-1}(a)} = \frac{1}{2}\frac{a^2/4}{b+}\frac{a^2/4}{b+1+}\frac{a^2/4}{b+2+} \tag{44}$$

In this simulation study, the following expression for the radical exit coefficient, used by Rawlings and Ray,[30] was used:

$$k_{de} = (3D_m k_{trm}/k_p)/(D_m \mathrm{MW}_m/\rho_M k_p \Phi + r^2) \tag{45}$$

where D_m is the effective diffusivity of the monomeric radical inside the particle (cm^2/s) and k_{trm} is the rate coefficient for chain transfer to the monomer ($cm^3\ mol^{-1}\ s^{-1}$).

The increase in the polymerization rate with increased conversion is well known and is called *autoacceleration* or the *Trommsdorff effect*. The increase in the polymerization rate is due to diffusional limitations causing a decrease in k_t. At sufficiently high conversion, k_p also decreases. In this study, the following expression for k_t, given by Liotta[31] was used:

$$k_t = k_{t0} \exp(-19 w_p^{2.1}) \text{ when } w_p \le 0.75 \tag{46}$$

$$k_t = (0.707 w_p^3 + 1.886 w_p^2 + 1.67 w_p + 4.96) \times 10^9 \text{ when } w_p \ge 0.75$$

where k_{t0} is the termination rate constant in the particles without the gel effect ($cm^3\ mol^{-1}\ s^{-1}$) and w_p is the weight fraction of the polymer in the particles, which is given by the following equation:

$$w_p = (1 - \Phi) \times \rho_p/[\Phi\rho_M + (1 - \Phi)\rho_p] \tag{47}$$

MODELING PARAMETERS

Table I lists the values of the various parameters used in this study and the references from which they were taken.

NUMERICAL IMPLEMENTATION

The first-order explicit Euler method was used to integrate the ordinary differential equations with a time step of 10 s. IMSL MATH/LIBRARY version 3.0 Fortran subroutine ZREAL (Absoft Corp., Rochester Hills, MI), which uses the Muller method, was used to solve the nonlinear algebraic equation to obtain the value of the monomer volume fraction inside the particles. As already stated, the continued fraction form developed by Ugelstad et al.[29] was

TABLE I
Values of the Parameters Used in the Simulations

	Reference Source
$MW_M = 104.15$ g/mol	32
$\rho_M = 0.906$ g/cm^3	32
$\rho_p = 1.04$ g/cm^3	33
$\Phi_{sat} = 0.6$	34
$[M]_{sat} = 2.6 \times 10^{-6}$ g mol cm^{-3}	24
$k_p = 212,000$ cm^3 g mol^{-1} s^{-1} (at 50°C)	2
$k_{pw} = k_p$	This study
$k_{t0} = 6.52 \times 10^{16} \exp(-8870/R_GT)$ cm^3 g mol^{-1} s^{-1}	30
$k_{tw} = k_{t0}$	This study
$k_{trm} = 7 \times 10^{-5} k_p$	30
$D_m = 7.1 \times 10^{-11}$ cm^2/s	30
$MW_E = 288.33$ g/mol	
$[E]_{cmc} = 0.0005$ g/cm^3 (at 50°C)	2
$a_{em} = a_{ep} = 35 \times 10^{-16}$ cm^2/molecule	2
$MW_I = 270.33$ g/mol	35
$k_d = 1.8 \times 10^{17} \exp(-34,100/R_GT)$	36
$f = 0.5$	
$k_{mp} = 28$	24
$k_{mm} = \varepsilon k_{mp}$	
$\varepsilon = 0.08$	1, this study
$\varepsilon = 0.01$ (when radical exit is considered in aqueous-phase radical balance)	
$\chi = 0.692$ (detailed model[1] and model 1)	1, this study
$\chi = 0.45$ (models 2, 3, and 4)	This study
$\chi = 0.15$ (model 5)	This study
$\gamma = 32$ dyne/cm	2
$\beta = 0$ (detailed model,[1] models 1 and 2)	1, this study
$\beta = 6 \times 10^{-23}$ (number of particles)$^{-1}$ s^{-1} (model 3)	This study
$\beta = 50 \times 10^{-23}$ to 800×10^{-23} (number of particles)$^{-1}$ s^{-1} (model 4)	This study
$\beta = 60 \times 10^{-23}$–$1000 \times 10^{-23}$ (number of particles)$^{-1}$ s^{-1} (model 5)	This study

$[E]_{cmc}$, critical micelle concentration (g/cm^3); MW_I, molecular weight of the initiator (g/mol).

used to evaluate the average number of radicals per particle.

RESULTS AND DISCUSSION

Role of the radical exit and aqueous-phase termination in the aqueous-phase radical balance

The version of the lumped model used to evaluate the assumptions of neglecting radical exit and aqueous-phase radical termination in the aqueous-phase radical balance from the detailed, population balance model developed previously[1] was the same as the previous model. Hence, only micellar nucleation was included. Also, the Morton effect from the thermodynamic equation for monomer partitioning [eq. (36)] or the first term in that equation was neglected. This version of the lumped model is referred to as model 1 in this article. Different submodels for aqueous-phase radical balance were included one by one. These are summarized in Table II. RAD1 included radical generation due to initiator decomposition, radical entry into the micelles, and particles and neglected radical exit and termination; RAD2 included radical generation due to initiator decomposition, radical entry into the micelles, and particles and radical termination and neglected radical exit; RAD3 included radical generation due to initiator decomposition, radical entry into the micelles, and particles and radical exit and neglected termination of the aqueous-phase radicals; and RAD4 contained all of the terms. The value of χ was chosen as 0.692 to give a value for the saturated monomer volume fraction of $\Phi_{sat} = 0.6$ when monomer droplets were present or the aqueous phase was saturated with the monomer. This value of Φ_{sat} was given by Gardon.[34]

First, the predictions for the total number of particles formed were considered with model 1 and various submodels for the aqueous-phase radical

TABLE II
Summary of the Various Aqueous-Phase Radical Balance Submodels

Submodel	Initiator decomposition	Radical entry	Radical exit	Radical termination
RAD1	Yes	Yes	No	No
RAD2	Yes	Yes	No	Yes
RAD3	Yes	Yes	Yes	No
RAD4	Yes	Yes	Yes	Yes

TABLE III
Comparison of the Experimental Values of the Total Number of Particles Formed with the Detailed Model[1] and Model 1 with Different Aqueous-Phase Radical Balance Submodels

[E] (g/L of water)	Experimental value of N_P ($\times 10^{17}$/L of water)	Detailed model (RAD1, $\varepsilon = 0.08$)	Model 1 (RAD1, $\varepsilon = 0.08$)	Model 1 (RAD2, $\varepsilon = 0.08$)	Model 1 (RAD3, $\varepsilon = 0.01$)	Model 1 (RAD4, $\varepsilon = 0.01$)
1.88	1.8	1.76	2.08	2.08	1.74	1.58
3.13	2.2	2.61	2.82	2.82	2.66	2.49
6.25	4.0	4.17	4.29	4.29	4.94	4.76
12.5	6.0	6.49	6.82	6.82	9.45	9.28
25.0	10.0	9.97	10.51	10.51	18.44	18.27

balance. These are given in Table III. Also given are the experimental values and the predictions of the detailed model.[1] The amounts of initiator (potassium persulfate), monomer (styrene), and water for all of these runs were 1.25 g, 500 g, and 1000 cm^3, respectively. Model 1 with RAD1 and RAD2 predicted the same values. Hence, we concluded that the inclusion of aqueous-phase radical termination had no effect and could safely be neglected. Further, with the inclusion of radical exit (RAD3 and RAD4), the inclusion of aqueous-phase radical termination had an insignificant effect. Also, the inclusion of radical exit (RAD3 and RAD4) led to lower values of ε ($= k_{mm}/k_{mp}$) and higher values of the total number of particles formed. ε had to be lowered to provide a close match at the lowest emulsifier concentration. With the inclusion of radical exit, the aqueous-phase radical concentration increased; this resulted in a larger number of nucleated particles. The exclusion of radical exit (RAD1 and RAD2) gave a number of particles close to the experimental values. Hence, we concluded that radical exit should not have contributed to the aqueous-phase radical balance. Probably, the exited hydrophobic monomeric radicals are not able to penetrate the hydrophilic exterior of the micelles and participate in particle nucleation.

In Table IV, the experimental values of conversion at the end of nucleation (X_n) at different emulsifier concentrations are compared with the predictions of model 1 with different submodels for the aqueous-phase radical balance. The inclusion of the aqueous-phase radical termination had no or an insignificant effect and could be safely neglected. However, the inclusion of radical exit led to an improvement in the predicted values.

The experimental values of the duration of the nucleation period (t_n) are compared with the predicted values in Table V. Model 1 with the inclusion and exclusion of the radical termination predicted similar values. Hence, we concluded again that the aqueous-phase radical termination had no effect on the model predictions and could be safely neglected. Further, the inclusion of radical exit led to much lower and closer values of the duration of the nucleation period. Only the exclusion of radical exit led to closer predictions to the experimental values of the duration of the nucleation period. Thus, radical exit had to be excluded from the aqueous-phase radical balances.

The predictions of model 1 for the variation of the monomer volume fraction inside the particles with time are given in Figure 1. The monomer volume fraction inside the particles was constant at 0.6 during intervals I and II because of the continuous supply of monomer from the droplets to the particles. Once the droplets disappeared, the monomer volume fraction in the polymer particle started decreasing with time. The time when it started to decrease (the end of interval II) increased with decreasing emulsifier concentration. A lower number of particles or reaction sites was formed as the emulsifier concentration decreased, and therefore, the monomer droplets existed for a longer period.

TABLE IV
Comparison of the Experimental Values of the Conversion at the End of the Nucleation with the Detailed Model[1] and Model 1 with Different Aqueous-Phase Radical Balance Submodels

[E] (g/L of water)	Experimental value of X_n	Detailed model (RAD1, $\varepsilon = 0.08$)	Model 1 (RAD1, $\varepsilon = 0.08$)	Model 1 (RAD2, $\varepsilon = 0.08$)	Model 1 (RAD3, $\varepsilon = 0.01$)	Model 1 (RAD4, $\varepsilon = 0.01$)
1.88	—	0.005	0.0080	0.0080	0.0095	0.0098
3.13	0.005	0.012	0.0151	0.0151	0.0165	0.017
6.25	0.03	0.03	0.0352	0.0352	0.0342	0.035
12.5	0.06	0.073	0.0817	0.0817	0.0698	0.070
25.0	0.146	0.173	0.1837	0.1837	0.141	0.142

TABLE V
Comparison of the Experimental Values of the Duration of the Nucleation Period with the Detailed Model[1] and Model 1 with Different Aqueous-Phase Radical Balance Submodels

[E] (g/L of water)	Experimental value of t_n (min)	Detailed model (RAD1, $\varepsilon = 0.08$)	Model 1 (RAD1, $\varepsilon = 0.08$)	Model 1 (RAD2, $\varepsilon = 0.08$)	Model 1 (RAD3, $\varepsilon = 0.01$)	Model 1 (RAD4, $\varepsilon = 0.01$)
1.88	—	3.67	4.33	4.33	5.67	7.00
3.13	5.1	5.39	6.00	6.00	6.57	7.58
6.25	9.2	8.59	9.16	9.16	7.50	8.11
12.5	12.5	13.36	13.83	13.83	8.18	8.53
25.0	18.0	19.45	20.00	20.00	8.70	8.88

Roles of the inclusion of individual radical balances, homogeneous nucleation, and Morton effect in the thermodynamic equation

Model 1 was extended to include individual radical balances; this was necessary for including homogeneous nucleation in the model. Also, the Morton effect, or the first term in eq. (36), was included. The value of interfacial tension was chosen as 32 dyne/cm, as reported by Harada et al.[2] for the nucleation period. A value of χ was chosen as 0.45 to predict that the droplets disappear at 43% conversion for the lowest emulsifier concentration, as reported by Harada et al.[2] The value of 0.45 for χ was close to the value of 0.43 reported by Morton et al.[26] and Gardon[34] for styrene monomer and its homopolymer. This choice of χ also ensured that the predicted values of Φ were less than $\Phi_{sat} = 0.6$, as reported by Harada et al.[2]

Because radical exit was not considered to contribute to the aqueous-phase radical balance, the balances for M_1, M_2, M_3, M_4, and M_5 were not included. This version of the model is referred to as model 2.

The number of particles formed due to homogeneous nucleation was negligible compared to those formed from micellar nucleation. The number of particles formed at the lowest emulsifier concentration of 1.88 g/L by homogeneous nucleation was 3042 compared to 3.97×10^{17} formed by micellar nucleation. Also, the contributions of R_2, R_3, R_4, and R_5 to the overall aqueous-phase radical balance were negligible compared to that of R_1. Near the beginning of the run (at 8 min), R_1, R_2, R_3, R_4, and R_5 were 7.27×10^5, 701, 6.76×10^{-2}, 6.52×10^{-6}, and 6.28×10^{-10}, respectively. We inferred from the simulation results that at all times, $R_1/R_{tot} \approx 1$, and the remaining ratios (R_2/R_{tot}, R_3/R_{tot}, R_4/R_{tot}, and R_5/R_{tot}) were approximately 0. Hence, homogeneous nucleation could be safely neglected for the reaction system and for the reaction conditions simulated in this study. Also, the individual radical balances need not be written. Because $R_1 \approx R_{tot}$, only the balance for the radical concentration generated by the decomposition of initiator should be considered. For the sake of generality, homogeneous nucleation and individual radical balances were included in this and further versions of the model.

The values of the duration of nucleation, conversion at the end of the nucleation period, and total number of particles formed at different emulsifier concentrations as predicted by model 2 are given in Table VI. Model 2 overpredicted the number of particles formed compared to model 1. The deviation between the predictions of model 2 for the number of particles formed and the experimental value is also given in Table VI as a difference between these two quantities. The deviation increased as the emulsifier concentration increased. The deviation occurred because, with the inclusion of the Morton effect, the value of the monomer volume fraction inside the particles decreased below 0.6 during the nucleation period, as predicted by model 1 (cf. Figs. 1 and 2). Hence, the particles grew at a slower rate, and as a result, the consumption of emulsifier to stabilize the growing particle surface area also occurred at a slower rate. Therefore, micelles existed in the

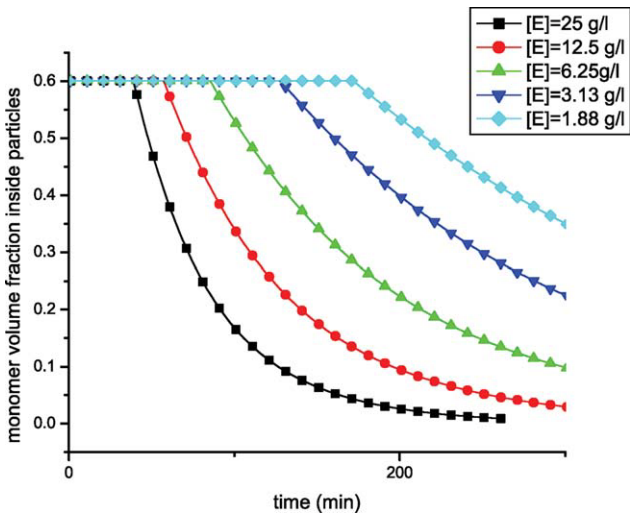

Figure 1 Prediction of model 1 for the variation of monomer volume fraction inside the particles with time at different emulsifier concentrations. [Color figure can be viewed in the online issue, which is available at wileyonlinelibrary.com.]

TABLE VI
Predictions of Model 2 for the Duration of Nucleation Period, Conversion at the End of the Nucleation Period, and Total Number of Particles Formed

[E] (g/L of water)	t_n (min)	X_n	N_P ($\times 10^{17}$/L of water)	$(N_P^{\text{Model2}} - N_P^{\text{exp}})$ ($\times 10^{17}$/L of water)
1.88	5.50	0.0087	3.97	2.17
3.13	7.16	0.0168	5.49	3.29
6.25	10.16	0.0348	9.03	5.03
12.5	14.83	0.741	15.9	9.90
25.0	23.00	0.1521	29.96	19.96

reaction medium for a longer time; this resulted in the higher number of particles predicted by model 2 as compared to model 1. Higher predicted values of the number of particles suggested that coagulation should be included in the model. Also, the extent of coagulation should increase with increasing the emulsifier concentration.

As shown in Figure 2, with decreasing emulsifier concentration, the value of Φ increased because larger particles existed in the system at a given time.

Role of inclusion of coagulation

Initially, the coagulation was considered to occur throughout the course of polymerization. We found the value of β by fitting of the predicted value of the total number of particles formed at the highest emulsifier concentration to the experimental value. The value of β so obtained was 6.0×10^{-23} L (number of particles)$^{-1}$ s^{-1}. This value of β was kept the same for all of the emulsifier concentrations. This version of the model is referred to as model 3. The predictions of model 3 for the various variables are given in Table VII. As shown, they were in good agreement with the experimental values.

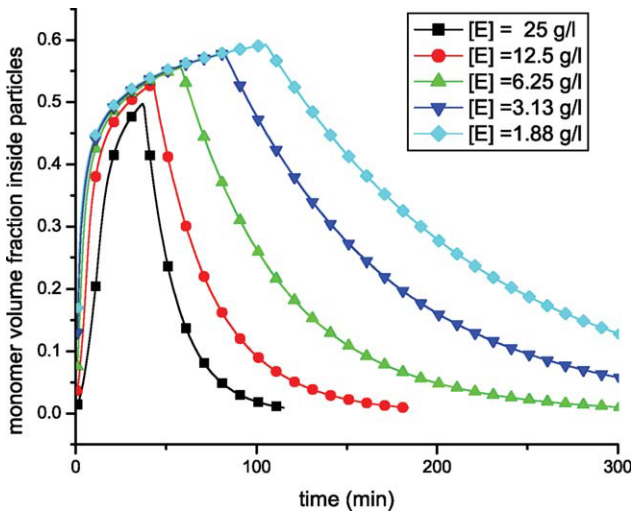

Figure 2 Prediction of model 2 for the variation of monomer volume fraction inside the particles with time at different emulsifier concentrations. [Color figure can be viewed in the online issue, which is available at wileyonlinelibrary.com.]

Harada et al.[2] reported that the number of particles was constant after the cessation of nucleation or after interval I. Recently, Carro et al.[37] also reported the same finding. Also, Carro et al.[37] reported that there was coagulation during interval I and its extent increased with increasing emulsifier concentration. The experimental conditions were the same in these two studies. Thus, coagulation throughout the course of polymerization was ruled out. It was included only during the nucleation period. Hence, the number of particles were allowed to change during interval I only until the time when area of the micelles become zero. The values of β were adjusted to give a close match between the predicted values and the experimental values of the number of particles formed at each emulsifier concentration. The predicted values are given in Table VIII for different emulsifier concentrations. Also, the values of β are given. This version of the model is referred to as model 4.

The value of β increased with decreasing emulsifier concentration. This was expected because the particles were likely to be more unstable at the lower emulsifier concentrations. Further, the model now overpredicted the values of the duration of nucleation and the conversion at the end of the nucleation period. Thus, micelles existed in the system for a longer period. We believed that the duration of the nucleation period could be reduced if the particles were allowed to grow at a faster rate than what was predicted by model 3. In model 4, the

TABLE VII
Predictions of Model 3 for the Duration of the Nucleation Period, Conversion at the End of the Nucleation Period, and Total Number of Particles Formed

[E] (g/L of water)	t_n (min)	X_n	N_P ($\times 10^{17}$/L of water)
1.88	5.66	0.0092	1.52
3.13	7.167	0.0159	2.09
6.25	10.33	0.0357	3.39
12.5	15.16	0.0763	5.82
25.0	23.83	0.1616	10.08

TABLE VIII
Predictions of Model 4 for the Duration of the Nucleation Period, Conversion at the End of the Nucleation Period, and Total Number of Particles Formed

[E] (g/L of water)	t_n (min)	X_n	N_P ($\times 10^{17}$/L of water)	β
1.88	8.667	0.0124	1.83	800×10^{-23}
3.13	11.667	0.0228	2.33	500×10^{-23}
6.25	15.33	0.0478	4.07	210×10^{-23}
12.5	23.33	0.1083	5.90	110×10^{-23}
25.0	34.16	0.2332	9.82	50×10^{-23}

value of χ was taken as 0.45, as was the case with models 2 and 3. This value was lowered to 0.15 at this point to allow a higher monomer volume fraction inside the particles and, thereby, increase their rate of growth during the early times. The value of Φ was 1 in the micelles, and as soon as the nucleation started, it did not drop to 0.6, as was the case in model 1, or to a very low value, as was the case with models 2, 3 and 4. The value of Φ in the newly formed particles was between 1 and what was predicted by the various models so far. The lowering of χ allowed us to account for this. This version of the model with coagulation during the nucleation period and $\chi = 0.15$ is referred to as model 5. The predictions of this model are given in Table IX. Also, the new values of β are given. As shown, the predicted values were in good agreement with the experimental values. The predictions of model 5 for the variation of monomer volume fraction inside the particles with time for different emulsifier concentrations are plotted in Figure 3. As shown, higher values of Φ were predicted compared those predicted with model 2.

Both model 1 (with micellar nucleation, no coagulation, and no consideration of Morton's effect) and model 5 (with micellar and homogeneous nucleation, coagulation during the nucleation stage, and consideration of Morton Effect) gave good agreement with the experimental values of the various variables considered. However, they predicted different profiles of change in the number of particles

TABLE IX
Predictions of Model 5 for the Duration of Nucleation Period, Conversion at the End of the Nucleation Period, and Total Number of Particles Formed

[E] (g/L of water)	t_n (min)	X_n	N_P ($\times 10^{17}$/L of water)	β
1.88	6.16	0.0099	1.78	1000×10^{-23}
3.13	8.00	0.0172	2.38	600×10^{-23}
6.25	10.66	0.0371	4.12	250×10^{-23}
12.5	16.33	0.0832	6.00	140×10^{-23}
25.0	23.66	0.1715	10.80	60×10^{-23}

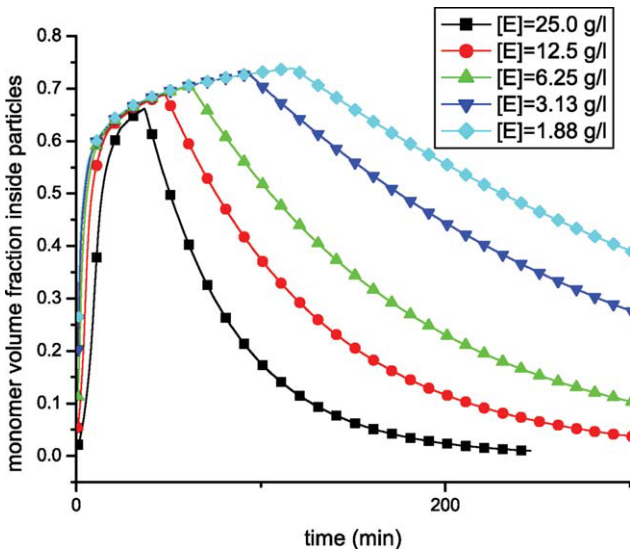

Figure 3 Prediction of model 5 for the variation of monomer volume fraction inside the particles with time at different emulsifier concentrations. [Color figure can be viewed in the online issue, which is available at wileyonlinelibrary.com.]

formed with time. Model 1 predicted that the number of particles formed would increase with time until the end of nucleation and reach a constant value thereafter. This is shown in Figure 4. Model 5 predicted that the number of particles formed would pass through a maximum during the nucleation period. The height of the maxima increased with increasing emulsifier concentration. This is shown in Figure 5. As the model 5 predictions were supported by the recent findings of Carro et al.,[37] model 5 was taken as the one representing the reality.

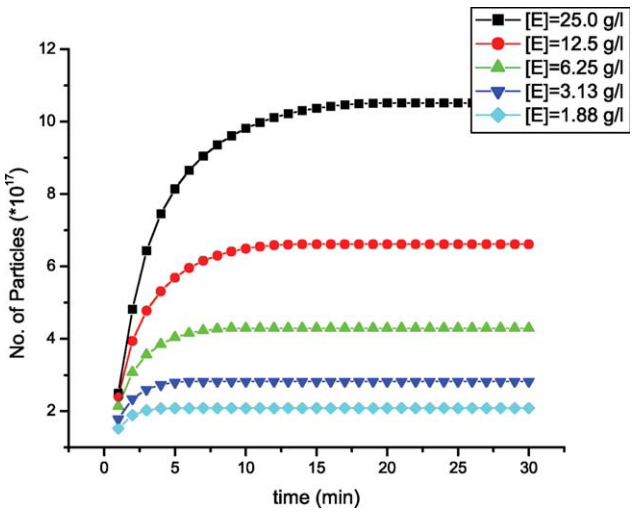

Figure 4 Prediction of model 1 for the variation of the number of particles formed with time for different emulsifier concentrations. [Color figure can be viewed in the online issue, which is available at wileyonlinelibrary.com.]

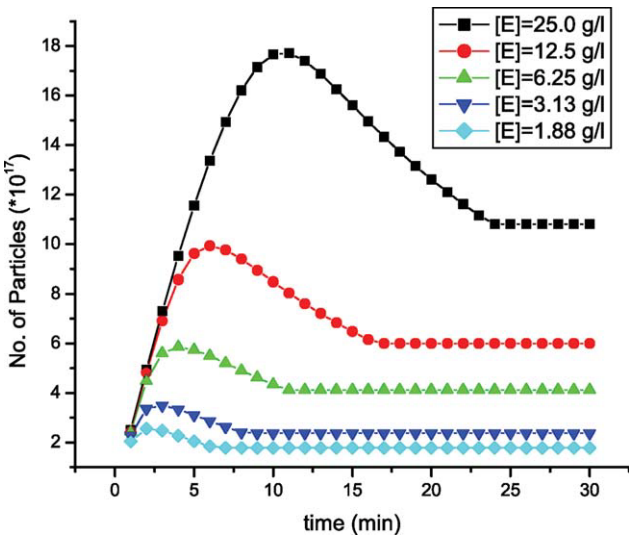

Figure 5 Prediction of model 5 for the variation of the number of particles formed with time for different emulsifier concentrations. [Color figure can be viewed in the online issue, which is available at wileyonlinelibrary.com.]

CONCLUSIONS

The aim of this study was to develop and validate a lumped model for emulsion polymerization that incorporated all complex, competing processes. Initially, the roles of aqueous-phase radical termination and radical exit were evaluated. We found that the inclusion of aqueous-phase termination had either no or an insignificant effect on the variables chosen for model validation, namely, the duration of nucleation, conversion at the end of the nucleation period, and total number of particles formed. Hence, it could be safely neglected. The inclusion of radical exit in the aqueous-phase radical balance greatly enhanced particle nucleation, and hence, the total number of particles formed was overpredicted. It also resulted in a decrease in the duration of the nucleation period. Only when it was not included in the model did the predictions for the aforementioned variables come into good agreement with the experimental values. For this reason, it was not included thereafter in the aqueous-phase radical balance. Probably, the exited hydrophobic monomeric radicals are never able to penetrate the hydrophilic exterior of the micelles and participate in particle nucleation.

Next, we evaluated the roles of individual radical balances and homogeneous nucleation. It was found that contributions of oligomeric radicals to the overall radical balance were negligible. Also, the number of particles nucleated by homogeneous nucleation was insignificant compared to the number of those nucleated by micellar nucleation. The effect of the inclusion of Morton effect in the thermodynamic equation for monomer distribution among various phases was evaluated. We found that with the inclusion of this effect, the number of particles formed was overpredicted. This led to the inclusion of coagulation in the model.

Initially, coagulation was thought to occur throughout the course of polymerization. With a single value of β, found by the fitting of the predicted value of the number of particles at the highest emulsifier concentration to the experimental value, we found that the predicted values of all the variables for different emulsifier concentrations were close to their experimental values. However, on the basis of the experimental results of Harada et al.[2] and Carro et al.,[37] which showed that the number of particles were constant after the cessation of nucleation or after interval I, and the results of Carro et al.,[37] in which coagulation occurred for all of the emulsifier concentrations only during interval I, coagulation was included during interval I only. The values of β at different emulsifier concentrations were found by the fitting of the predicted values of the number of particles formed to the experimental values. These values were found to increase with decreasing emulsifier concentrations and were in the range 10^{-23} to 10^{-20} L (number of particles)$^{-1}$ s^{-1}. The value of χ had to be lowered from 0.43 to 0.15 to provide a better fit of the predicted variables to their experimental values. Model 5, with micellar and homogeneous nucleation and coagulation during the nucleation period and with the Morton effect considered, should be considered the one closest to reality.

A number of areas for future studies have emerged from this study and include emulsifier adsorption and desorption kinetics, coagulation kinetics, kinetics of monomer transport during the early stages, which must include micellar monomer transport also, and the role of radical exit in affecting the aqueous-phase radical balance and, hence, nucleation kinetics.

NOMENCLATURE

a	parameter accounting for the relative importance of radical entry with respect to radical termination
a_{em}	emulsifier surface coverage area on the micelles (cm^2/molecule)
A_m	total surface area of the micelles (cm^2)
A_{m0}	total initial surface area of the micelles (cm^2)
A_P	total particle surface area (cm^2)
b	parameter accounting for the relative importance of radical exit with respect to radical termination inside the particle
D_m	effective diffusivity of the monomeric radical inside the particle (cm^2/s)
$[E]_{cmc}$	critical micelle concentration (g/cm^3)

[E] emulsifier concentration (g/l)
f initiator decomposition efficiency
F_i number of particles containing i radicals
i average number of radicals per particle
$I_b(a)$ modified Bessel function of the first kind of order b and argument a
[I] initiator concentration (mol/cm^3)
$[I]_W$ initiator concentration in the aqueous phase (mol/cm^3)
k_d initiator decomposition rate constant (s^{-1})
k_{de} radical exit coefficient (s^{-1})
k_e radical entry rate coefficient (s^{-1})
k_{mm} mass-transfer coefficient of radical entry into the micelles (cm^{-2} s^{-1})
k_{mp} mass-transfer coefficient of radical entry into the particles (cm^{-2} s^{-1})
k_p propagation rate constant in the particles (cm^3 mol^{-1} s^{-1})
k_{pw} propagation rate constant in the aqueous phase (cm^3 mol^{-1} s^{-1})
k_t radical termination rate constant inside the particles (cm^3 mol^{-1} s^{-1})
k_{t0} termination rate constant in the particles without the gel effect (cm^3 mol^{-1} s^{-1})
k_{trm} rate coefficient for chain transfer to the monomer (cm^3 mol^{-1} s^{-1})
k_{tw} termination rate constant in the aqueous phase (cm^3 mol^{-1} s^{-1})
M total aqueous-phase concentration of radicals derived from exited radicals (mol/cm^3)
m_e mass of the emulsifier in the reaction medium (g)
M_i aqueous-phase concentration of a radical with chain length i derived from the exited radical (mol/cm^3; $i = 1, 2, 3, 4,$ or 5)
MW_E molecular weight of the emulsifier (g/mol)
MW_I molecular weight of the initiator (g/mol)
MW_M molecular weight of the monomer (g/mol)
$[M]_{aq}$ monomer concentration in the aqueous phase (mol/cm^3)
$[M]_D$ monomer concentration in the droplets (mol/cm^3)
$[M]_P$ monomer concentration in the particles (mol/cm^3)
$[M]_R$ monomer concentration in the reaction medium (mol/cm^3)
$[M]_{sat}$ monomer concentration at saturation in the aqueous phase (mol/cm^3)
N_A Avogadro's number
N_{m0} initial number moles of the monomer (mol)
N_P total number of particles formed
$[P]_R$ polymer concentration in the reaction medium (mol/cm^3)
r radius of the particle (cm)
R total aqueous-phase concentration of radicals derived from the initiator decomposition (mol/cm^3)
R_{coag} rate of coagulative nucleation (s^{-1})
r_{dry} unswollen or dry particle radius (cm)
R_{em} rate of radical entry into the micelles (s^{-1})
R_G universal gas constant (cal mol^{-1} K^{-1})
R_{hom} rate of homogeneous nucleation (s^{-1})
R_i total aqueous-phase concentration of a radical with chain length i derived from the initiator decomposition (mol/cm^3; $i = 1, 2, 3, 4,$ or 5)
R_{nuc} rate of nucleation (s^{-1})
R_P rate of polymerization (mol/s)
R_{tot} total aqueous-phase radical concentration (mol/cm^3)
t time (s)
T absolute temperature (K)
t_n duration of the nucleation period (s)
V_D volume of the droplets (cm^3)
v_P volume of a particle (cm^3)
V_P volume of the particles (cm^3)
V_R volume of the reaction medium (cm^3)
V_W volume of the aqueous phase (cm^3)
w_p weight fraction of the polymer in the particles
X conversion
X_n conversion at the end of nucleation

Greek letters

β coagulation rate constant (number of particles)$^{-1}$ s^{-1}
ε k_{mm}/k_{mp}
γ interfacial tension (dyne/cm)
χ Flory–Huggins interaction parameter
Φ monomer volume fraction inside the particles
Φ_{sat} saturated monomer volume fraction inside the particles
ρ_M density of the monomer (g/cm^3)
ρ_p density of the polymer (g/cm^3)

References

1. Sood, A. J Appl Polym Sci 2008, 9, 1403.
2. Harada, M.; Nomura, M.; Kojima, H.; Eguchi, W.; Nagata, S. J Appl Polym Sci 1972, 16, 811.
3. Chern, C. S. Prog Polym Sci 2006, 31, 443.
4. Harkins, W. D. J Chem Phys 1945, 13, 381.
5. Harkins, W. D. J. Chem Phys 1946, 14, 47.
6. Smith, W. V.; Ewart, R. H. J Chem Phys 1948, 16, 592.
7. Priest, W. J. J Phys Chem 1952, 56, 1077.
8. Jacobi, B. Angew Chem 1952, 64, 539.
9. Fitch, R. M.; Tsai, C. H. In Polymer Colloids; Fitch, R. M., Ed.; Plenum: New York, 1971; p 73.
10. Hansen, F. K.; Ugelstad, J. J Polym Sci Polym Chem Ed 1978, 16, 1953.
11. Maxwell, I. A.; Morrison, B. R.; Napper, D. H.; Gilbert, R. G. Macromolecules 1991, 24, 1629.

12. Lichti, G.; Gilbert, R. G.; Napper, D. H. J Polym Sci Polym Chem Ed 1983, 21, 269.
13. Feeney, P. J.; Napper, D. H.; Gilbert, R. G. Macromolecules 1984, 17, 2520.
14. Hansen, F. K.; Ugelstad, J. In Emulsion Polymerization; Piirma, I., Ed.; Academic: New York, 1982.
15. Gardon, J. L. J Polym Sci Part A-1: Polym Chem 1971, 9, 2763.
16. Sood, A. Indian Chem Eng 2002, 44, 75.
17. Sood, A. J Appl Polym Sci 2004, 92, 2884.
18. Sood, A.; Awasthi, S. K. Macromol Theory Simul 2004, 13, 603.
19. Sood, A.; Awasthi, S. K. Macromol Theory Simul 2004, 13, 615.
20. Tauer, K.; Nozari, S.; Imroz Ali, A. M. Macromolecules 2005, 38, 8611.
21. Hernandez, H. F.; Tauer, K. Ind Eng Chem Res 2007, 46, 4480.
22. Brooks, B. W. British Polym J 1970, 2, 197.
23. Brooks, B. W. British Polym J 1971, 3, 269.
24. Min, K. W.; Ray, W. H. J Macromol Sci Polym Rev 1974, 11, 177.
25. Min, K. W.; Ray, W. H. J Appl Polym Sci 1978, 22, 89.
26. Morton, M.; Kaizerman, S.; Altier, M. W. J Colloid Sci 1954, 9, 300.
27. Stockmayer, W. H. J Polym Sci 1957, 24, 314.
28. O'Toole, J. T. J Polym Sci Part C: Polym Symp 1969, 27, 171.
29. Ugelstad, J.; Mork, P. C.; Aasen, J. O. J Polym Sci Part A-1: Polym Chem 1967, 5, 2281.
30. Rawlings, J. B.; Ray, W. H. Polym Eng Sci 1988, 28, 257.
31. Liotta, V. Ph.D. Thesis, Lehigh University, 1996.
32. Fleischer, D. In Polymer Handbook, 3rd ed.; Brandrup, J., Immergut, E. H., Eds.; Wiley-Interscience: New York, 1989.
33. Rudd, J. F. In Polymer Handbook, 3rd ed.; Brandrup, J., Immergut, E. H., Eds.; Wiley-Interscience, New York, 1989.
34. Gardon, J. L. J Polym Sci Part A-1: Polym Chem 1968, 6, 2859.
35. CRC Handbook of Chemistry and Physics, 62nd ed.; Weast, R. C., Ed.; CRC: Boca Raton, FL, 1981.
36. Koltoff, I. M.; Miller, I. K. J Am Chem Soc 1951, 73, 3055.
37. Carro, S.; Herrera-Ordonez, J.; Castillo-Tejas, J. J Polym Sci Part A: Polym Chem 2010, 48, 3152.